Clinical Neurophysiology 120 (2009) 360–373

Contents lists available at ScienceDirect

Clinical Neurophysiology

journal homepage: www.elsevier.com/locate/clinph

Auditory-evoked potentials to frequency increase and decrease of high- and low-frequency tones

Hillel Pratt [a,*], Arnold Starr [b], Henry J. Michalewski [b], Andrew Dimitrijevic [b], Naomi Bleich [a], Nomi Mittelman [a]

[a] Evoked Potentials Laboratory, Behavioral Biology, Gutwirth Building, Technion – Israel Institute of Technology, Haifa 32000, Israel
[b] Neurology Research Laboratory, University of California – Irvine, Irvine, CA 92697, USA

ARTICLE INFO

Article history:
Accepted 24 October 2008
Available online 12 December 2008

Keywords:
Event-related potentials
Spectral change
Frequency resolution
Change complex
Source estimation
Functional imaging

ABSTRACT

Objective: To define cortical brain responses to large and small frequency changes (increase and decrease) of high- and low-frequency tones.
Methods: Event-Related Potentials (ERPs) were recorded in response to a 10% or a 50% frequency increase from 250 or 4000 Hz tones that were approximately 3 s in duration and presented at 500-ms intervals. Frequency increase was followed after 1 s by a decrease back to base frequency. Frequency changes occurred at least 1 s before or after tone onset or offset, respectively. Subjects were not attending to the stimuli. Latency, amplitude and source current density estimates of ERPs were compared across frequency changes.
Results: All frequency changes evoked components P_{50}, N_{100}, and P_{200}. N_{100} and P_{200} had double peaks at bilateral and right temporal sites, respectively. These components were followed by a slow negativity (SN). The constituents of N_{100} were predominantly localized to temporo-parietal auditory areas. The potentials and their intracranial distributions were affected by both base frequency (larger potentials to low frequency) and direction of change (larger potentials to increase than decrease), as well as by change magnitude (larger potentials to larger change). The differences between frequency increase and decrease depended on base frequency (smaller difference to high frequency) and were localized to frontal areas.
Conclusions: Brain activity varies according to frequency change direction and magnitude as well as base frequency.
Significance: The effects of base frequency and direction of change may reflect brain networks involved in more complex processing such as speech that are differentially sensitive to frequency modulations of high (consonant discrimination) and low (vowels and prosody) frequencies.

1. Introduction

1.1. Auditory change detection

Sensory systems are tuned to detect changes in the environment so the organism can take appropriate action to survive. Neural mechanisms underlying the processing of pitch changes of a tone have been studied in humans using auditory cortical potentials (McCandless and Rose, 1970; Kohn et al., 1978; Arlinger et al., 1982; Yingling and Nethercut, 1983; Tervaniemi et al., 2005). In these studies the N_{100}/P_{200} components were evoked in response to changes of pitch and their amplitude could be related to both the magnitude of change and the expertise of the listener in discriminating these stimuli (Tervaniemi et al., 2005). Other studies examined N_{100} and P_{200} to changes in continuous stimuli such as music (Jones et al., 1998; Jones and Perez, 2001, 2002) or speech (Laufer and Pratt, 2003a) that varied in one or more parameters (i.e., pitch or timbre) and designated them the "C(hange)-Complex", which in continuous stimuli is not confounded by onset responses to the appearance of the stimulus.

Humans require hearing to communicate through oral speech and language, acoustic patterns that vary over time in frequency and intensity. A particular hallmark of speech sounds is rapid changes in frequency that determine the identity of the speech element, regardless of the absolute value of frequency or intensity (e.g., /du/ spoken by a loud soprano or by a soft base). During development, the auditory system is trained and tuned to frequency *variations* in sounds. The ability to discriminate successive sounds on the basis of frequency is central to the perception of different formants (peak energy bands) of vowels and frequency peaks of consonants (Medwetzky, 2002) and is termed frequency

* Corresponding author. Tel.: +972 4 8292321; fax: +972 4 8295761.
E-mail address: hillel@tx.technion.ac.il (H. Pratt).

1388-2457/$34.00 © 2008 International Federation of Clinical Neurophysiology. Published by Elsevier Ireland Ltd. All rights reserved.
doi:10.1016/j.clinph.2008.10.158

resolution. The N_{100} and P_{200} have been studied in response to acoustic changes in natural speech associated with phonemes and transitions: fricative to vowel (Ostroff et al., 1998; Friesen and Trembley, 2006), vowel to vowel (Martin and Boothroyd, 2000) and vowel to fricative (Laufer and Pratt, 2003a), and to change in non-speech sounds (Harris et al., 2007, 2008).

1.2. Frequency mapping in the auditory system

The discrimination of speech components utilizes different ranges of acoustic frequencies. For instance, consonant discrimination depends primarily on high-frequency hearing whereas vowels and prosody of speech depend on the low frequencies and amplitude modulations of speech. The neural encoding of low and high frequencies differ along the ascending auditory pathway, utilizing the 'volley principle', reflecting temporal cues, and the 'place principle', reflecting the site of origin of cochlear activation. The temporal pattern of firing of some auditory nerve units (particularly those encoding low frequencies) follows the stimulus waveform in a 'phase locked' manner up to frequencies of about 4–5 kHz in the auditory nerve (Rose et al., 1968; Palmer and Russel, 1986) and antero-ventral cochlear nucleus (Goldberg and Brownell, 1973) of experimental animals. In humans, measures of the frequency following response that reproduce low frequency tones (Moushegian et al., 1973) as well as psychoacoustic studies (Javel and Mott, 1988) suggest a sharp decline in phase locking in the ascending auditory pathway, beginning at about 1 kHz. In the real world, cortical neurons are rarely activated by tones, and when exposed to tones, the tone frequency is changing (Whitfield and Evans, 1965). The general consensus is that although the auditory cortex tends to be tonotopically organized, it also processes a variety of other aspects of sound such as its source in space (Brugge and Merzenich, 1973; Palmer, 1995).

Electrophysiological, neuromagnetic, and fMRI studies of auditory cortex in humans have shown that frequency sensitivity is bilaterally localized on the supratemporal plane, with low frequencies more lateral and anterior than high frequencies (Pantev et al., 1988, 1995; Verkindt et al., 1995). However, some studies failed to find tonotopic mapping of N_{100} and its magnetic counterpart N_{100m} and reported other factors, such as latency, to be important (Roberts and Poeppel, 1996; Stufflebeam et al., 1998; Lutkenhoner et al., 2003). In addition, several complications render the fixed single dipole source used in most studies 'simplistic' (Lutkenhoner, 2003). For example, intracerebral recordings (Godey et al., 2001) indicate that N_{100} and its magnetic counterpart N_{100m} are generated by multiple cortical generators. Intracerebral recordings indicate that N_{100m} is generated by several non-primary auditory areas on the lateral aspects of Heschl's gyrus and planum temporale ('belt'), only some of which are tonotopically organized. However, when the temporal complexity of N_{100m} is taken into account, and analysis is conducted on single-subject data to minimize variability, source estimation supports N_{100m} tonotopic organization in auditory cortex (Lutkenhoner et al., 2003). Based on the multiple cortical generators of N_{100} and their possible tonotopic organization in both primary ('core') and secondary ('belt') auditory cortices, N_{100} to frequency change would be expected to have a distributed and possibly non-stationary source.

1.3. ERPs to frequency change

In a previous study (Dimitrijevic et al., 2008) Event-Related Potentials (ERPs) to brief (100 ms) frequency increases in a continuous tone were studied. Potentials had amplitudes and latencies that were significantly more affected by the magnitude of low than of high-frequency change. Furthermore, dipole sources of N_{100} revealed an orderly location shift with the magnitude of low but not high-frequency change. These results indicate that cortical components to brief increases of frequency during low and high continuous tones differ. However, the brain activity that was measured in that study was a composite of responses to the frequency increase and the immediately following decrease, and hence in the present study low- and high-frequency changes were studied separately for increase and decrease.

Processing of frequency increase and decrease is most likely different. As a result of the Doppler effect, frequency increase of an auditory object may indicate its movement toward the listener, while frequency decrease is compatible with its movement away from the listener. In the processing of speech prosody, frequency increase and decrease are different, implying a query (increase) vs command (decrease). The associated brain activity is therefore likely to differ between frequency increase and decrease. In the present study, we separated increase from decrease to allow studying their potentials separately. In the short frequency increases of our previous study increase always preceded frequency decrease, so this order was maintained in the present study. In this way the results of this study could be compared with the earlier results without being confounded by the preceding frequency change direction.

In our previous study, brief (100 ms) increases in frequency of an otherwise continuous tone, were presented monaurally. In the present study we used tone bursts lasting a few seconds, to correspond to the globally segmented acoustics of speech, while retaining the single feature change of frequency increase or decrease. Frequency increase and decrease were separated by one second intervals so the potentials to frequency increase and decrease could be studied separately. In our previous study stimuli were presented monaurally, possibly resulting in larger cortical activation contralateral to the stimulated ear. In the present study we used binaural stimuli to avoid confounding lateralization of brain activity with lateralization of stimulus presentation.

1.4. Purpose of this study

The purpose of this study was to define the auditory-evoked potentials to frequency increase and decrease of binaural high- and low-frequency tones. Furthermore, we estimated sources of these potentials with no assumptions on their number and location. We hypothesized that the potentials to frequency increase would be distinct and larger than to frequency decrease, and that these potentials will be greater to large than to small frequency change. These effects would be larger to low- than to high-base frequency.

2. Methods

2.1. Subjects

Sixteen (13 men and 3 women) 18–24 years old right-handed normal hearing subjects participated in the study. Fifteen of them (13 men and 2 women) were found to have technically acceptable data (low enough levels of eye blinks and myogenic noise) and were subsequently included in the analysis. Subjects were paid for their participation and all procedures were approved by the Institutional Review Board for experiments involving human subjects (Helsinki Committee).

2.2. Stimuli

Low- and high-frequency binaural tone bursts were randomly presented through earphones (Sony MDR-CD770) with a flat frequency response (within 10 dB across the frequency range

100–10,000 Hz). Tones were presented at interstimulus intervals that randomly varied in the range between 500 and 600 ms. Intervals between tones were varied to avoid expectancy and to prevent predictability of the acoustic events. Binaural stimuli were used to avoid confounding lateralization of brain activity with lateralization of stimulus presentation. Fig. 1 depicts the time course of stimuli. Low-frequency tone bursts had a base frequency of 250 Hz which, after 1.0 or 1.3 s from burst onset, randomly increased by 10% or by 50% (to 275 or to 375 Hz). Frequency increase was followed, after 1 s, by a frequency decrease back to 250 Hz, followed by continuation of the 250 Hz base frequency for another 1.0 s (Fig. 1, top). Frequency change was abrupt (not ramped) and took place at zero crossing to minimize spectral splatter. The intensity of the sound throughout the stimulus was maintained at 65 dBnHL. Similarly, binaural 4000-Hz tone bursts included, after 1.0 or 1.3 s from onset (to diminish expectancy of the change), a 10% or a 50% frequency increase (to 4400 or to 6000 Hz), followed after 1.0 s by a return to the base frequency of 4000 Hz for another second, with no change in intensity. Frequency splatter was minimal as evidenced by no audible 'click'. Moreover, detailed acoustic analysis of the stimuli revealed no evidence of significant frequency splatter in such frequency changes (Dimitrijevic et al., 2008). Moreover, spectral splatter is expected to be larger with the larger frequency change, and in particular with high base frequency (due to the larger and more abrupt amplitude transient) and this would have resulted in shorter evoked potential latency due to the associated increase in intensity. In contrast, our results showed that frequency increase evoked components that were actually later for the large (50%) than for the small (10%) increase from the high-(4000 Hz) base frequency.

Interstimulus intervals and pre-change base frequency durations were varied to avoid predictability of the timing of changes. In addition, for each base frequency (250 and 4000 Hz) there was a no-change stimulus in which a 2.2-s duration of the base frequency was presented without change. The no-change tones were included to reduce the predictability of a change. In all, there were 10 stimuli: (2 pre-change durations × 2 change magnitudes + no change condition) × 2 base frequencies, which were randomly presented during the recording session, with equal probability (10%). Each stimulus was presented 240 times.

2.3. Procedure

Twenty-two 9-mm silver disc electrodes were placed according to the 10–20 system at: F_{p1}, F_7, F_3, F_z, F_4, F_8, F_{p2}, T_3, C_3, C_z, C_4, T_4, T_5, P_3, P_z, P_4, T_6, O_1, and O_2, 1.5 cm above the left and right mastoids (M'_1 and M'_2), as well as below the left eye, referenced to F_z, to control for eye movements (EOG). The mastoidal electrodes were placed above their standard positions to avoid distortion in the source estimation procedures. In total, EEG was recorded from 21 electrodes referenced to the center of the chin and EOG was recorded from one diagonal differential recording below the left eye referenced to F_z. An electrode over the 7th cervical spinous process served as ground. Note that this montage is different than the average common reference montage of our previous study (Dimitrijevic et al., 2008). Impedance at each electrode was maintained below 5 kΩ.

Subjects were then seated in a comfortable reclining armchair in a sound-proof chamber and instructed to read a complicated text (on which they were subsequently examined) while stimuli were presented (not attending to sounds). The diverted attention of subjects from the auditory stimuli, as well as the randomness of frequency changes and their timing were designed to reduce endogenous contributions to the brain potentials. Subjects were allowed breaks as needed. The total duration of a typical recording session was 4–5 h consisting of 16–20 recording segments with breaks between them.

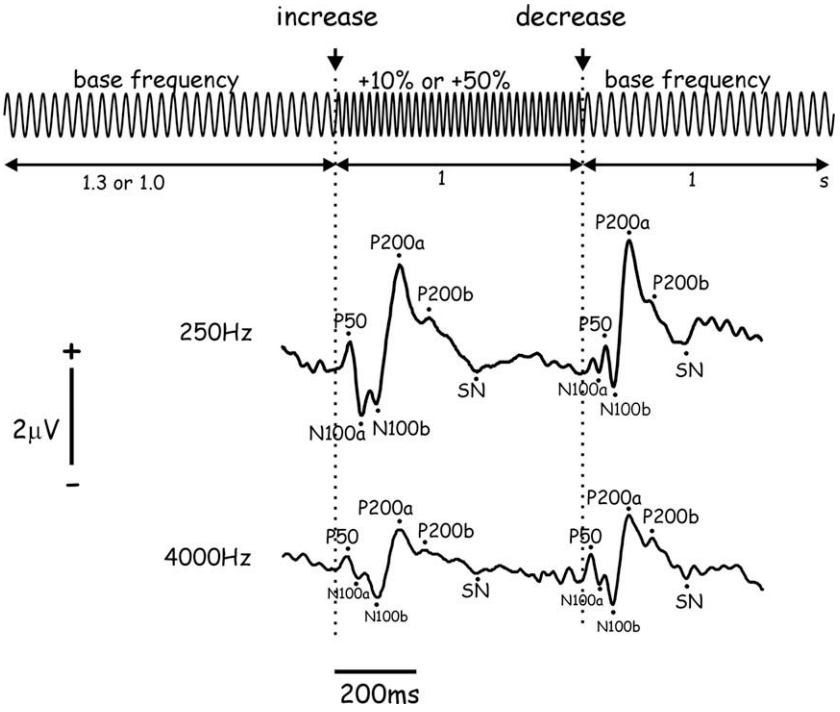

Fig. 1. Time courses of the binaural stimuli and the ERP waveforms evoked by them. Stimuli consisted of tone bursts with base frequencies of 250 or 4000 Hz during which a frequency increase of 50% or 10% (first vertical dotted line), followed by decrease back to the base frequency (second vertical dotted line), took place. Brain potentials were recorded in response to the frequency increase and to the decrease. Waveforms to frequency increase and decrease of 50% are presented in this figure at the respective times relative to the stimulus. The components analyzed in this study are indicated on the waveforms.

2.4. Data acquisition

Potentials from the EEG (100,000×) and EOG (20,000×) channels were amplified, digitized with a 12-bit A/D converter at a rate of 256 samples/s, filtered (0.1–100 Hz, 6 dB/octave slopes) and stored for offline analysis. EEG processing began with segmentation of the continuous EEG to epochs beginning 100 ms before until 1000 ms after each frequency increase or decrease, separately. Eye movement correction (Attias et al., 1993) and artifact rejection (±150 μV) followed segmentation. Average waveforms were then computed separately for frequency increase and frequency decrease (Fig. 1, bottom) for the 10% and 50% changes in the 250- and 4000-Hz tone bursts. Corresponding frequency changes preceded by 1.0 and 1.3 s of base frequency were found indistinguishable in preliminary testing based on 5 subjects. Therefore, changes preceded by 1.0 and 1.3 s of base frequency were averaged together, resulting in approximately 350 repetitions contributing to the potentials evoked by each direction of frequency change (increase or decrease) for each combination of base frequency (250 and 4000 Hz) and change magnitude (10% and 50%). These eight separate averages (2 direction of changes × 2 base frequencies × 2 change magnitudes) were computed for each subject, as well as across subjects to obtain grand mean waveforms. After averaging, the data were low-pass filtered (FIR rectangular filter with a low-pass cutoff at 20–24 Hz) and baseline (average amplitude across the 100 ms before stimulus onset) corrected.

2.5. ERP waveform analysis

ERP analysis included peak latency and amplitude comparisons among stimulus types as well as comparisons of the respective source current densities. P_{50} was defined as the positive peak in the range of 25–90 ms, preceding N_{100} which was the most negative peak or bifid peak, between 80 and 150 ms. P_{200} was defined between 140–220 ms and was often double-peaked with the second peak between 210 and 280 ms. P_{200} was followed by a slow negativity (SN) which spanned latencies between 300 and up to 900 ms from frequency change. Group grand-averaged ERPs for each condition determined the latency ranges for peak identification.

ERP peak amplitudes and latencies were subjected to a repeated measures analysis of variance (ANOVA) with Greenhouse–Geisser correction for violation of sphericity and Bonferroni corrections for multiple comparisons. In addition to peak latency and amplitude, the slow negativity (SN) was also assessed by the average amplitude between its peak and 900 ms after the frequency change. This measure avoided distortions of the component's area by possible overlap with preceding components such as P_{200b}. Potentials to frequency increase and frequency decrease were separately analyzed using repeated measures analysis of variance, for the effects of the following factors: Base frequency (250 and 4000 Hz), Change magnitude (10% and 50% change) and 11 of the Electrodes (F_3, F_z, F_4, C_3, C_z, C_4, P_3, P_z, P_4, T_3, and T_4) representing frontal, central, parietal and temporal scalp areas. Comparison of the effects of frequency increase and decrease was conducted separately for high- and low-base frequencies using repeated measures analysis of variance for the effects of the following factors: Direction of change (increase, decrease from base frequency), Change magnitude (10% and 50% change) and 11 of the Electrodes (same as above). Probabilities below 0.05, after Greenhouse–Geisser corrections, were considered significant.

2.6. ERP functional imaging

Standardized Low-Resolution Electromagnetic Tomographic Analysis (sLORETA, Pascual-Marqui et al., 1994; Pascual-Marqui, 2002) was applied on the 21-channel ERP records to image the estimated source current density throughout the duration of P_{50}–N_{100}–P_{200}–SN in response to the eight frequency changes and to compare the current density distributions among stimulus conditions.

sLORETA is a functional brain imaging method that estimates the distribution of current density in the brain as suggested by the minimum norm solution (Pascual-Marqui, 2002) and applied to a boundary element head model (Fuchs et al., 2002). The minimum norm solution used in this implementation assumes the three-dimensional current distribution to have minimum overall intensity, employing weighting strategies to favor superficial sources and standardized current densities. Localization inference is based on standardized values of the current density estimates. The solution space is restricted to cortical gray matter and hippocampus. A total of 6430 voxels at 5 mm spatial resolution are registered to the Stereotaxic Atlas of the Human Brain (Talairach and Tournoux, 1988). While this source estimation technique narrows the infinite number of possible solutions to a unique estimate – it is still just an estimate based on assumptions. The results must therefore be treated with caution, particularly regarding the spatial resolution of the method which is low by the very nature of the method. In this study, differences in current density distributions associated with the frequency changes were assessed using Statistical non-Parametric Mapping (SnPM). The SnPM method estimates the probability distribution by using a randomization procedure, corrects for multiple comparisons and has the highest possible statistical power (Nichols and Holmes, 2002). The SnPM method in the context of ERP source estimation was validated in our previous studies by comparing its results with more conventional ANOVA results (Laufer and Pratt, 2003b; Sinai and Pratt, 2003).

Specifically, in this study we used the 'pseudo-*t*' statistic which reduced noise in the data by averaging over adjacent voxels (Nichols and Holmes, 2002). In order to trace time segments of significant differences between responses we compared them on a time-frame-by-time-frame, voxel-by-voxel basis for the duration of the analysis period. A time-segment was designated significant only if it contained at least five contiguous significant ($P < 0.05$) time-frames. We employed this procedure to reduce the probability that time-frames assigned with significance by chance alone due to alpha inflation would be included in the analysis. Average *t*-values were then obtained across the contiguous significant time-frames to obtain a single image consisting of 6430 voxels representing the entire time segment. The procedure outlined above was employed in order to trace significant time segments, utilizing the high temporal resolution of sLORETA, while extending (to the time domain) the method originally used by Nichols and Holmes (2002), of averaging significant *t*-values over space only.

3. Results

Frequency changes evoked clear components, beginning with a P_{50}, followed by N_{100} and P_{200} which were double peaked at bilateral- and right-temporal sites, respectively, and a late slow negativity – SN (Figs. 2 and 3). Latencies of the second of the double-peaked N_{100} and P_{200} had variabilities that were often twice as large as those of the first peak (Table 1) and thus the double peaking of these components is not always evident in the grand averages of Figs. 2 and 3. Descriptive statistics of the latencies and amplitudes of the peaks evoked by the large (50%) frequency change are listed in Table 1.

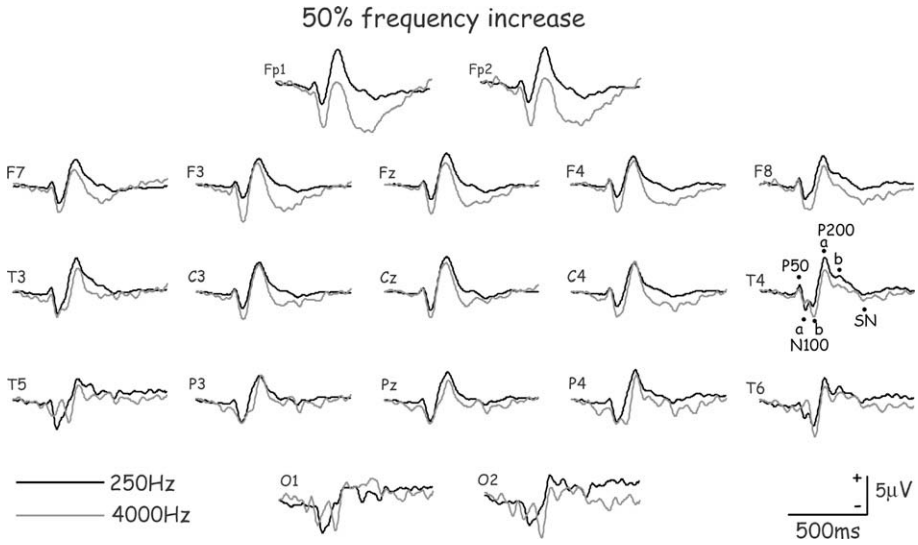

Fig. 2. Scalp distribution of the potentials to the large (50%) frequency increase from the high-(4000 Hz) and low-(250 Hz) base frequencies. Grand average across 15 subjects. The plots include a baseline of 100 ms before the frequency increase.

3.1. Evoked potentials to frequency increase

Frequency increase evoked components that were, in general, larger and earlier for the large (50%) than for the small (10%) increase from the low-(250 Hz) base frequency, while from the high-base frequency (4000 Hz) they were also larger but later for the large compared to the small frequency increase (Table 1 and Fig. 4). The details follow.

3.1.1. Waveform analysis

P_{50}, N_{100a}, and N_{100b} latencies to frequency increase were significantly affected by the magnitude of frequency change [$F(1,14) = 16.68$; $p < 0.002$ for P_{50}, $F(1,14) = 13.98$; $p < 0.003$ for N_{100a} and $F(1,14) = 5.45$; $p < 0.05$ for N_{100b}], and were longer to the small than to the large increase. P_{50} and N_{100a} amplitudes were significantly affected by base frequency [$F(1,14) = 6.31$; $p < 0.03$ for P_{50} and $F(1,14) = 12.28$; $p < 0.005$ for N_{100a}], with larger amplitudes to low frequency than to high frequency. N_{100a} amplitude was also affected by magnitude of the frequency increase [$F(1,14) = 13.95$; $p < 0.003$] and was larger to the 50% increase. Base frequency and magnitude of frequency increase interacted in their effects on N_{100a}amplitude [$F(1,14) = 13.71$; $p < 0.003$], which was significantly affected by the magnitude of increase only with the 250 Hz base frequency. N_{100b} latency was significantly [$F(1,14) = 14.06$; $p < 0.003$] longer to the 10% frequency increase from 4000 Hz. N_{100b} amplitude was significantly larger to the 50% frequency increase [$F(1,14) = 7.09$; $p < 0.02$].

P_{200a} latency was significantly affected by the magnitude of frequency increase [$F(1,14) = 6.34$; $p < 0.03$], being longer to the 10% increase, more so with the 250-Hz base frequency. This resulted in a significant base frequency × change magnitude interaction [$F(1,14) = 5.68$; $p < 0.05$]. In addition, a significant electrode × change magnitude interaction [$F(10,140) = 4.94$; $p < 0.001$] indicated that latency differences between electrodes

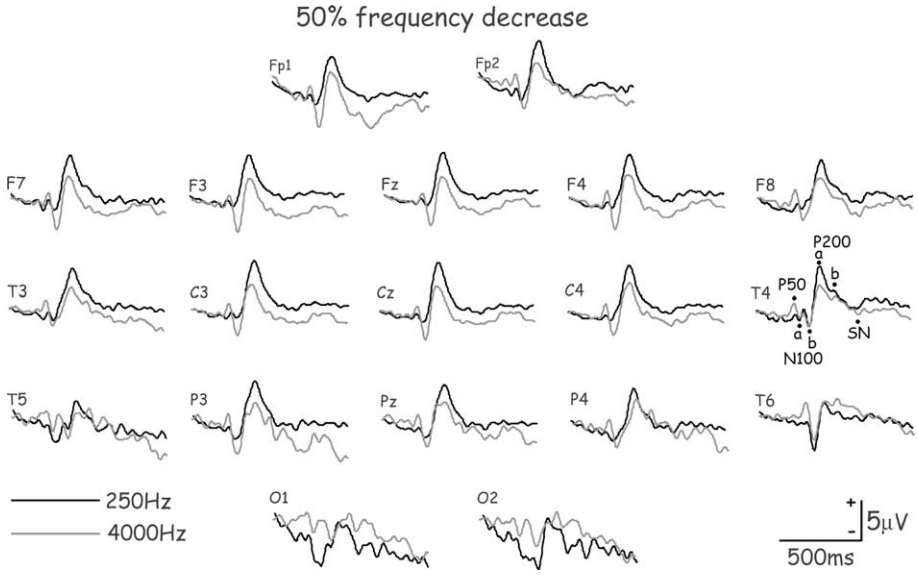

Fig. 3. Scalp distribution of the potentials to the large (50%) frequency decrease from the high-(4000 Hz) and low-(250 Hz) base frequencies. Grand average across 15 subjects. The plots include a baseline of 100 ms before the frequency decrease.

Table 1
Averages ± standard errors of mean latencies and amplitudes, SN average amplitude from its peak until 900 ms after the frequency change, as well as prevalence of components to 50% frequency increase and decrease from base frequencies of 250 and 4,000 Hz. Latencies are listed in ms, amplitudes in μV and incidence across 11 electrodes of all 15 subjects is in %. SN was always measured as the most negative point in the respective latency range.

	250-Hz Increase	250-Hz Decrease	4000-Hz Increase	4000-Hz Decrease
P_{50} Latency	42 ± 0.8	48 ± 1.8	40 ± 1.0	35 ± 1.0
Amplitude	0.65 ± 0.07	0.35 ± 0.07	0.18 ± 0.04	0.49 ± 0.05
Prevalence	92	100	99	100
N_{100a} Latency	85 ± 1.1	87 ± 1.7	85 ± 1.3	78 ± 1.1
Amplitude	−2.24 ± 0.10	−0.62 ± 0.09	−1.25 ± 0.09	−1.14 ± 0.08
Prevalence	100	92	94	96
N_{100b} Latency	116 ± 4.5	132 ± 1.8	144 ± 1.7	128 ± 2.2
Amplitude	−1.27 ± 0.09	−0.33 ± 0.07	−0.66 ± 0.08	−0.32 ± 0.07
Prevalence	56	67	90	76
P_{200a} Latency	195 ± 1.3	186 ± 1.2	200 ± 1.5	188 ± 2.3
Amplitude	3.74 ± 0.18	3.12 ± 0.15	1.32 ± 0.11	1.23 ± 0.08
Prevalence	99	100	99	100
P_{200b} Latency	257 ± 2.6	257 ± 2.0	258 ± 1.6	267 ± 2.3
Amplitude	2.02 ± 0.11	1.71 ± 0.11	0.35 ± 0.09	0.16 ± 0.05
Prevalence	67	95	88	89
SN Latency	461 ± 4.3	427 ± 4.8	426 ± 6.7	452 ± 3.8
Amplitude	−0.75 ± 0.08	−0.19 ± 0.07	−0.92 ± 0.08	−0.73 ± 0.07
Av. Amplitude	−0.23 ± 0.04	−0.36 ± 0.08	−0.36 ± 0.04	−0.29 ± 0.07

were larger with the larger frequency increase. P_{200a} and P_{200b} amplitudes were significantly larger to changes from the low than from the high-base frequency [$F(1,14) = 53.11$; $p < 0.001$ for P_{200a} and $F(1,14) = 50.26$; $p < 0.001$ for P_{200b}] and significantly larger to the larger frequency change [$F(1,14) = 30.22$; $p < 0.001$ for P_{200a} and $F(1,14) = 10.68$; $p < 0.01$ for P_{200b}]. In addition, significant electrode × change magnitude interactions on these peaks' amplitudes [$F(10,140) = 8.92$; $p < 0.001$ for P_{200a} and $F(10,140) = 3.75$; $p < 0.001$ for P_{200b}] indicated that amplitude differences between electrodes were larger with the larger frequency change and with changes from the low-base frequency.

SN peak amplitude was significantly larger with the high-base frequency [$F(1,14) = 6.55$; $p < 0.03$]. In addition, significant electrode × base frequency interactions [$F(10,140) = 3.16$; $p < 0.002$] indicated that SN latency differences between electrodes were larger with the higher base frequency.

3.1.2. Source current density estimates

Estimating the source current density of the scalp-recorded potentials to frequency increase revealed activity that peaked in a number of brain structures slightly (10–20 ms) later than the scalp-recorded voltage peaks. This systematic slight discrepancy was most likely due to the pattern of summation of partially overlapping intracranial fields to generate positive and negative peaks on the scalp. Fig. 5 shows the time courses of activation in key brain areas in the left and right hemispheres, estimated to be

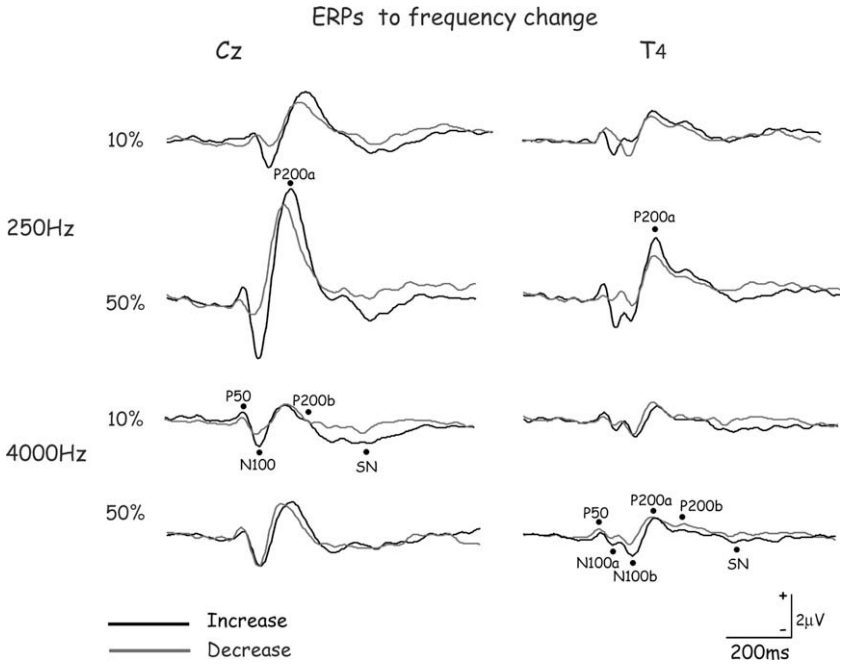

Fig. 4. Grand-averaged (15 subjects) waveforms of potentials to the eight frequency changes at C_z and T_4 (where double-peaked components were most evident): 10% and 50% increase and decrease from base frequencies of 250 and 4000 Hz. Note the larger amplitudes of potentials to changes from 250 Hz, compared to 4000 Hz, and to frequency increase compared to decrease. The plots include a baseline of 100 ms before the frequency change.

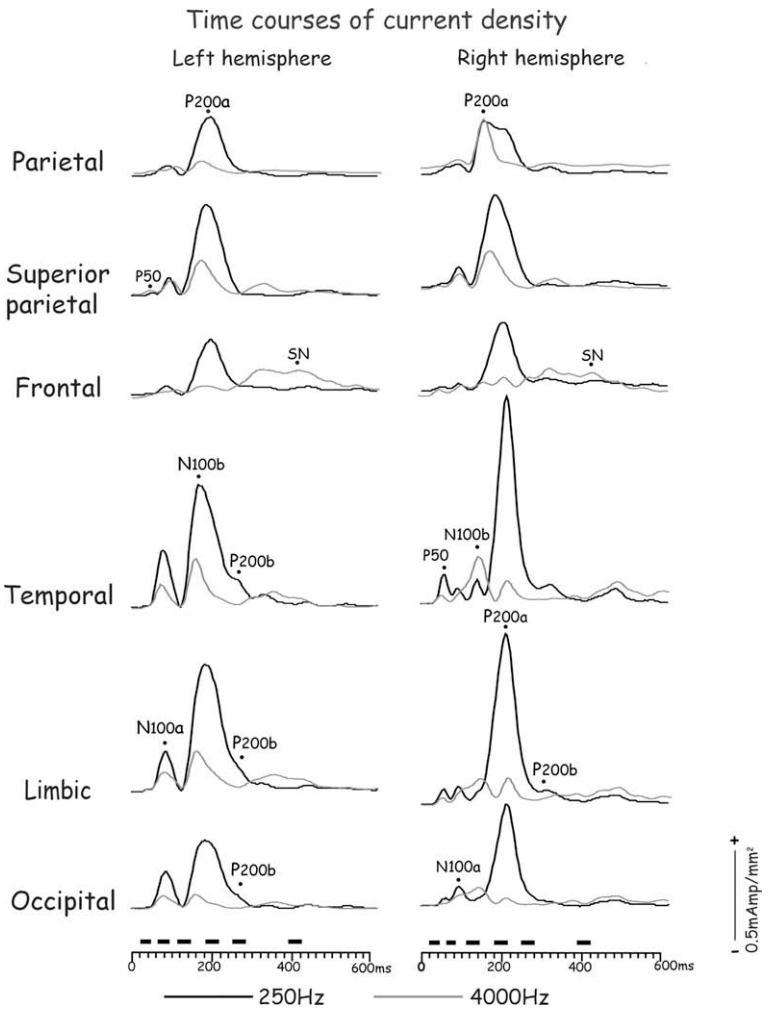

Fig. 5. Time courses of average current density values in the left and right hemisphere regions that were most involved with 50% frequency increase from high- and low-base frequencies. The horizontal bars above the timescale mark the ranges of P_{50}, N_{100a}, N_{100b}, P_{200a}, P_{200b}, and SN scalp-recorded peak latencies among subjects. Current density peaks are labeled according to their scalp-recorded counterparts. Time 0 corresponds to the frequency increase.

involved in the potentials to the large frequency increase from high- and low-base frequencies.

Source current density estimates for P_{50} were mostly localized to the right Temporal lobe area (in the vicinity of BA20, BA21, BA22, and BA38) for both the high- and low-base frequency. N_{100a} activity localized to the left Temporal lobe area (in the general area of BA20 and BA21) and to the right Frontal lobe (around BA25) and superior Temporal lobe (approximately at BA34 and BA28) with the high-base frequency. With the low-base frequency activity was mainly on the left at the Limbic lobe (in the area around BA36) and Temporal Lobe (generally around BA20 and BA21), as well as right Limbic areas (in the vicinity of BA23 and BA28) and right Frontal lobe (close to BA25). N_{100b} was associated with activity in the left Temporal lobe area (in the general location of BA39, BA20, and BA21) for the low-base frequency (Fig. 6, top) and at both left and right Temporal lobes (around BA20 and BA21) and in the vicinity of the Insula (BA13) for the high-base frequency.

P_{200a} activity was estimated to originate in some left and mostly right Limbic areas (in the general location of BA28, BA34, and BA36) for the low-base frequency (Fig. 6, bottom), while with the high-base frequency the right Limbic lobe (approximately at BA34) and both left and right Frontal lobes (around BA25) were involved. P_{200b} was associated with activation around left Insula (BA13) and left Temporal lobe (BA20 and BA21) by the low-base frequency and only in the vicinity of the right Frontal lobe (BA45) for the high-base frequency. SN peak activity was associated with frontal (in the general location of BA10, BA11, and BA25) activation, which was preceded by temporal (approximately at BA38) activation before the peak of SN.

Statistical non-parametric *t*-value mapping of current density differences between small and large frequency increase revealed, with the low-base frequency, a significant difference in current density during the time of N_{100b}, P_{200a} and P_{200b}, with higher current density to the larger frequency increase in the vicinity of the occipito-temporal junction and parietal areas. In addition, current densities during the time of P_{200a} and P_{200b} were higher to increase from the low-base frequency than from the high-base frequency. Even though they were prominent in opposite hemispheres, there were no significant differences in the current density distributions associated with N_{100a} and N_{100b}. Significant differences in current density distributions were found between P_{200a} and P_{200b} and between N_{100b} and P_{200a} with the low- base frequency, located for the small frequency increase to the vicinity of the Insula (BA13) and for the large frequency increase to midline Frontal areas (around BA9).

3.2. Evoked potentials to frequency decrease

Frequency decrease-evoked components that were larger and earlier for the 50% change than for the 10% change for both the

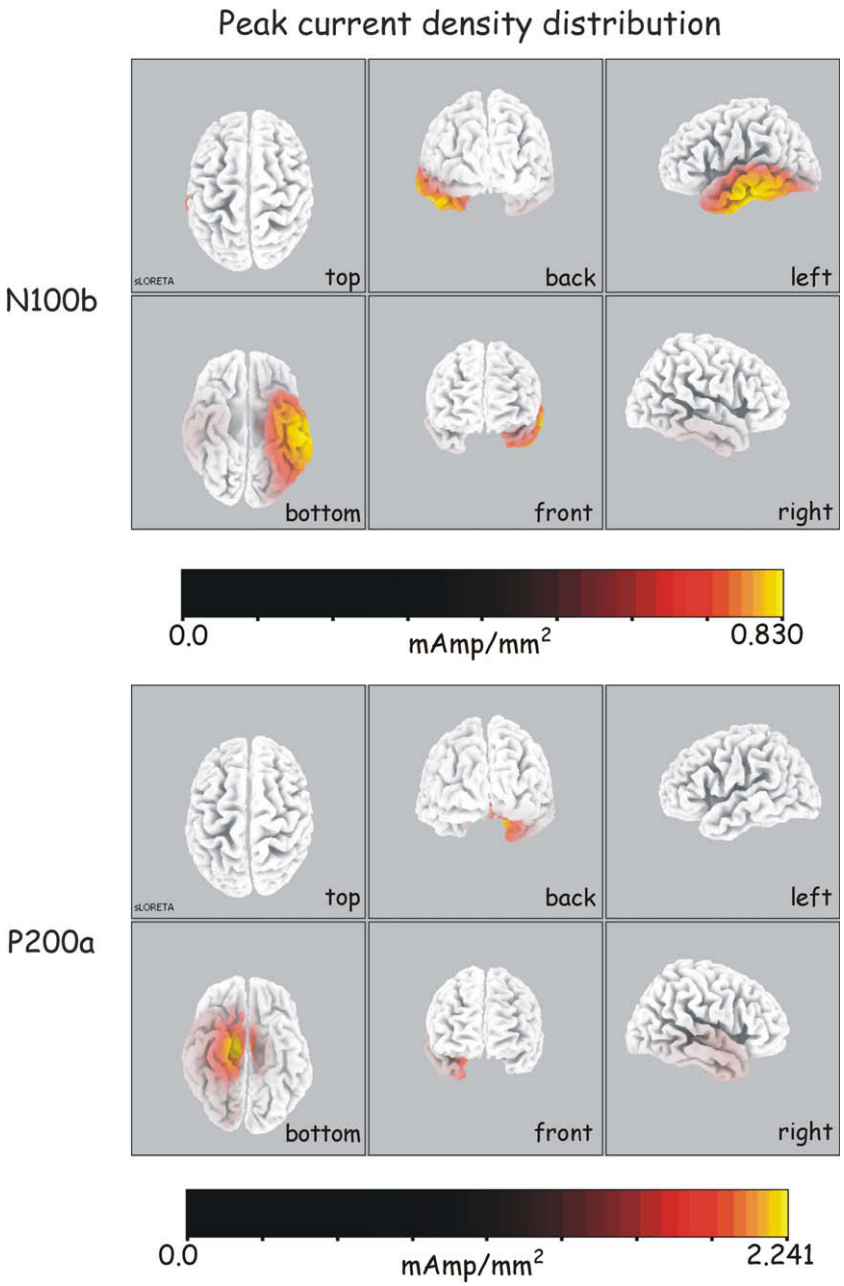

Fig. 6. Average source current density estimates associated with N_{100b} (top) and P_{200a} (bottom) to the 50% frequency increase from 250 Hz. Six views of the brain are presented for each component, as indicated on each view. N_{100b} activity involved mostly left Temporal lobe areas while P_{200a} was associated with some left but mostly right Limbic and Temporal activation.

low-base frequency and the high-base frequency (Fig. 4) as detailed below.

3.2.1. Waveform analysis

P_{50} and N_{100a} latencies to frequency decrease were significantly affected by the magnitude of frequency change [$F(1,14) = 22.81$; $p < 0.001$ for P_{50}, $F(1,14) = 16.94$; $p < 0.002$ for N_{100a}] and were longer to the small than to the large change. They were also affected by the base frequency [$F(1,14) = 31.82$; $p < 0.001$ for P_{50}, $F(1,14) = 13.46$; $p < 0.003$ for N_{100a}], with longer latencies to the low-base frequency. N_{100a} amplitude was significantly affected by base frequency [$F(1,14) = 5.29$; $p < 0.05$], with larger amplitudes to the high-base frequency. Base frequency and electrodes interacted in their effects on N_{100a} amplitude [$F(10,140) = 8.21$; $p < 0.001$], which varied more among electrodes with the high-base frequency.

P_{200a} latency was significantly longer to the 10% frequency decrease [$F(1,14) = 13.18$; $p < 0.003$]. Base frequency and electrodes interacted in their effects on P_{200a} latency [$F(10,140) = 2.4$; $p < 0.02$] such that latencies varied more among electrodes with the high-base frequency. P_{200a} amplitude was significantly larger to the 50% than to the 10% frequency decrease [$F(1,14) = 21.91$; $p < 0.001$] and to the lower base frequency [$F(1,14) = 24.95$; $p < 0.001$]. Base frequency and magnitude of frequency decrease interacted in their effects on P_{200a} amplitude [$F(1,14) = 14.12$; $p < 0.003$] and the effects of frequency change were more evident with low-base frequency. Amplitude differences among electrodes were more evident with the low-base frequency, resulting in a

significant base frequency × electrode interaction [$F(10,140) = 12.06$; $p < 0.001$]. Amplitude differences among electrodes were also larger with the larger frequency decrease manifesting in a significant change magnitude × electrode interaction [$F(10,140) = 10.89$; $p < 0.001$]. P_{200b} amplitude was significantly larger to the lower base frequency [$F(1,14) = 23.37$; $p < 0.001$]. Base frequency and magnitude of frequency decrease interacted in their effects on P_{200b} amplitude [$F(1,14) = 7.88$; $p < 0.02$] with more evident effects of frequency change with low-base frequency, in which the amplitude was larger with the large frequency decrease. Amplitude differences among electrodes were more evident with the low-base frequency resulting in a significant base frequency × electrode interaction [$F(10,140) = 15.19$; $p < 0.001$].

SN latency was significantly longer to the larger frequency decrease [$F(1,14) = 8.29$; $p < 0.02$]. SN peak amplitude [$F(1,14) = 10.40$; $p < 0.01$] and average amplitude from peak to 900 ms [$F(1,14) = 10.24$; $p < 0.01$] were both larger with the 4000-Hz base frequency and were both significantly affected by an interaction of base frequency and electrodes [$F(10,140) = 2.85$; $p < 0.003$ for SN peak amplitude and $F(10,140) = 2.39$; $p < 0.02$ for its average amplitude from peak to 900 ms], indicating different scalp distributions to low- and high-base frequency.

3.2.2. Source current density estimates

Similar to frequency increase, source current density of the scalp-recorded potentials to frequency decrease revealed activity that peaked in a number of brain structures slightly (10–20 ms) later than the scalp-recorded voltage peaks. However, during the peak of P_{200a} intracranial peaks of current density preceded the scalp peak by approximately 20 ms, probably due to the overlap with preceding N_{100b} activity that shortened the scalp-recorded P_{200a} peak latency.

Source current density estimates for P_{50} located mostly to the right Temporal lobe area (in the general location of BA38 and BA21) but a smaller activation was noted in the left Frontal lobe (around BA9) for the high-base frequency. For the low-base frequency both left and right areas were involved: in the vicinities of the left Precuneus (BA31), Limbic lobe (BA36) and right Temporal (BA21) and Frontal (BA47) lobes. N_{100a} was mostly associated with activation of bilateral Limbic areas (around BA36, BA28, and BA23), and the general locations of left Insula (BA13) and right Parietal cortex (BA7). The Frontal lobe (in the vicinity of BA25) was involved in response to the high-base frequency. With low-base frequency, bilateral Limbic lobe (approximately at BA36) and Temporal lobe (around BA21) activation was noted. N_{100b} involved the areas around right Temporo-Parietal lobe (BA40, BA41, and BA39) with low-base frequency and mainly right Temporo-Parietal area (around BA40) and bilateral Limbic lobe (in the general location of BA23) with high-base frequency.

P_{200a} peaked with current density around the left and right Limbic area (BA34) with the low-base frequency, and in the right Temporal lobe (approximately BA38 and BA21) with the high-base frequency. P_{200b} generators were estimated to the vicinity of left Limbic areas (BA28 and BA34) and the right Frontal lobe (BA45 and Ba10) with low-base frequency. In response to changes from the high-base frequency, sources were estimated at the approximate locations of left Temporal lobe (BA20), left Frontal Lobe (BA47), left Insula (BA13), right Limbic area (BA23), and Precuneus (BA31). SN peak activity was associated with midline Frontal (in the vicinity of BA10, BA11, and BA25) activity following temporal (around BA38) activation before the peak of SN.

Statistical non-parametric *t*-value mapping of current density differences between small and large frequency decrease revealed, with the low-base frequency, a significant difference in current density during the time of P_{200a}, with higher current density to the larger frequency decrease in the vicinity of the occipito-temporal junction. Significant differences were also noted between the low and the high-base frequencies which were limited to the large frequency decrease (in the right occipital and temporal areas). There were no statistically significant differences in the current density distribution between N_{100a} and N_{100b}. There were significant differences in current density distribution between P_{200a} and P_{200b} with the large frequency change from low-base frequency, mainly in the Cuneus and Precuneus.

3.3. Component comparisons between frequency increase and decrease

Components to frequency increase tended to have higher amplitudes and longer latencies than their counterparts to frequency decrease, but there were variations from this general tendency, depending on the magnitude of frequency change and base frequency (Fig. 4) as detailed below.

3.3.1. Waveform analysis

With the low-base frequency of 250 Hz, frequency decrease evoked significantly longer P_{50} latencies than frequency increase [$F(1,14) = 5.06$; $p < 0.05$]. N_{100a} amplitudes were significantly affected by direction of change [$F(1,14) = 40.93$; $p < 0.001$], and were larger to frequency increase than decrease. Amplitude differences between electrodes were more pronounced with frequency increase, resulting in a significant direction of change × electrode interaction for N_{100a} amplitude [$F(10,140) = 5.76$; $p < 0.001$]. N_{100b} latency was longer for frequency decrease [$F(1,14) = 5.20$; $p < 0.05$] and its amplitude was larger for frequency increase [$F(1,14) = 16.37$; $p < 0.002$]. N_{100b} amplitude was also affected by an interaction of direction of change and change magnitude [$F(1,14) = 7.09$; $p < 0.02$], and was larger to the 50% frequency increase but larger to the 10% change when it was a frequency decrease. The amplitude differences between change magnitudes were larger for the frequency increase than for the frequency decrease. In addition, a significant electrode × direction of change interaction [$F(10,140) = 5.74$; $p < 0.001$] resulted in more pronounced differences between electrodes with frequency decrease. SN peak latency was significantly longer to frequency increase than decrease [$F(1,14) = 7.28$; $p < 0.02$]. SN average amplitude from peak to 900 ms was significantly larger to frequency increase than decrease [$F(1,14) = 6.96$; $p < 0.02$], and it was significantly affected by an interaction of direction of change and electrodes [$F(10,140) = 6.97$; $p < 0.001$], indicating that scalp distribution differed between frequency increase and decrease, with a larger variability with frequency increase.

With the high-base frequency of 4000 Hz P_{50} amplitude was significantly affected by direction of change [$F(1,14) = 4.75$; $p < 0.05$] and was larger to frequency decrease. N_{100b} was significantly affected by direction of change and its latency was longer [$F(1,14) = 1712$; $p < 0.002$] and amplitude larger [$F(1,14) = 7.38$; $p < 0.02$] to frequency increase. P_{200a} latency was significantly longer to frequency increase [$F(1,14) = 7.18$; $p < 0.02$] while P_{200b} latency was significantly longer to frequency decrease [$F(1,14) = 6.66$; $p < 0.03$]. SN peak amplitude [$F(10,140) = 2.66$; $p < 0.006$] and the average amplitude from SN peak to 900 ms after frequency change [$F(10,140) = 2.35$; $p < 0.02$] were both affected by significant electrode by direction of change interactions, indicating a difference in scalp distribution between frequency increase and decrease.

3.3.2. Source current density estimates

Statistical non-parametric *t*-value mapping of current density differences between frequency increase and decrease revealed, for the small frequency change from 250 Hz a significantly larger

current density to frequency increase during the time of peak N_{100a} (Fig. 7) in right frontal areas (in the vicinity of BA10).

3.3.3. Source comparison of N_{100} to tone onset, frequency increase and frequency decrease

In our previous study (Dimitrijevic et al., 2008), continuous tones were used rather than tone bursts, and it was therefore difficult to relate the N_{100} to frequency changes to the N_{100} arising from tone bursts. In this study, we could compare the N_{100} to burst onsets and to frequency change in the same subject, to the same sounds. In a preliminary comparison of sources of tone burst onsets with the responses to frequency increase and decrease in the same bursts, using the grand-averaged waveforms from all 15 subjects, we found their source current distributions to be different (Fig. 8): While the main sources of N_{100} to both frequency change and burst onset were from the temporal lobe, N_{100a} to frequency change was more inferior-midline and somewhat more anterior in location than the burst onset N_{100} and frequency change N_{100b}.

3.4. Summary of results

Overall, both base frequency and direction of change affected potentials to frequency change and their scalp and intracranial distributions. Frequency increase-evoked components that were larger and earlier for the large (50%) than for the small (10%) increase from the low-(250 Hz) base frequency, and were larger but later for the large (50%) than for the small (10%) increase from the high-(4000 Hz) base frequency. Frequency decrease evoked components that were larger and earlier for the 50% change than for the 10% change for both the low-base frequency and the high-base frequency. Distributions of scalp potentials and of intracranial current density were also different between increase and decrease and differences were typically significant with the low – but not with the high-base frequency. Moreover, for N_{100b} latency both frequency increase and decrease were significant in their effects, but in opposite directions: with the low-base frequency latency was shorter to frequency increase, whereas with the high-base frequency latency was longer to frequency increase.

The intracranial sources of potentials to frequency change located mostly to Temporal, Temporo-Parietal and to a lesser degree to Limbic and Frontal lobes. The differences in intracranial activity to frequency increase and decrease were significant in right Frontal areas. The distribution of intracranial sources were also affected by base frequency and magnitude of change.

4. Discussion

In this study brain potentials to large and small (50% and 10%) frequency increase and decrease were compared when the frequency changes involved high-(4000 Hz) or low-(250 Hz) base frequency. All frequency changes evoked potentials that included a P_{50}, followed by N_{100} and P_{200} which were often double peaked, and a slow negativity (SN). The results showed differences between the effects of frequency increase and decrease on brain activity and its intracranial distribution as well as differences in the brain processing of changes from high- and low-base frequencies that were affected by the magnitude of change. In general, these findings confirm the results of our previous study on frequency change (Dimitrijevic et al., 2008), and in addition show some differences and a number of additional effects that provide further insights on brain processing of frequency change.

In this study, sLORETA was used for source estimation. While this method uses a minimal set of assumptions, the source estimate is only one possible solution, favored by its assumptions over an infinite number of possible solutions. As a consequence of the assumptions made in this method, particularly when only 21 electrodes are used, the spatial resolution of the estimated sources is quite low and the discussion of sources should relate to general cortical regions. The listing of Brodmann areas in this report is only provided as an indicator of the general area of estimated activity

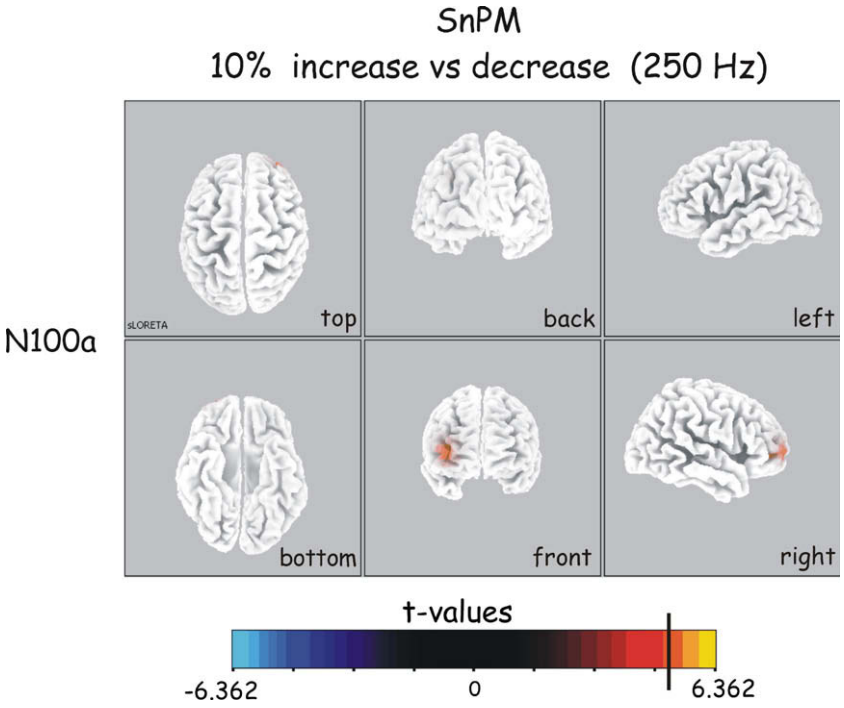

Fig. 7. Statistical non-parametric *t*-value mapping of current density of N_{100a} in response to the 10% frequency increase from 250 Hz compared to the respective current density to decrease back to 250 Hz. Six views of the brain are presented, as indicated on each view. The *t*-value for statistical significance is indicated by the vertical line on the color scale. The difference in current density between frequency increase and decrease was significant during N_{100a} in the right frontal lobe.

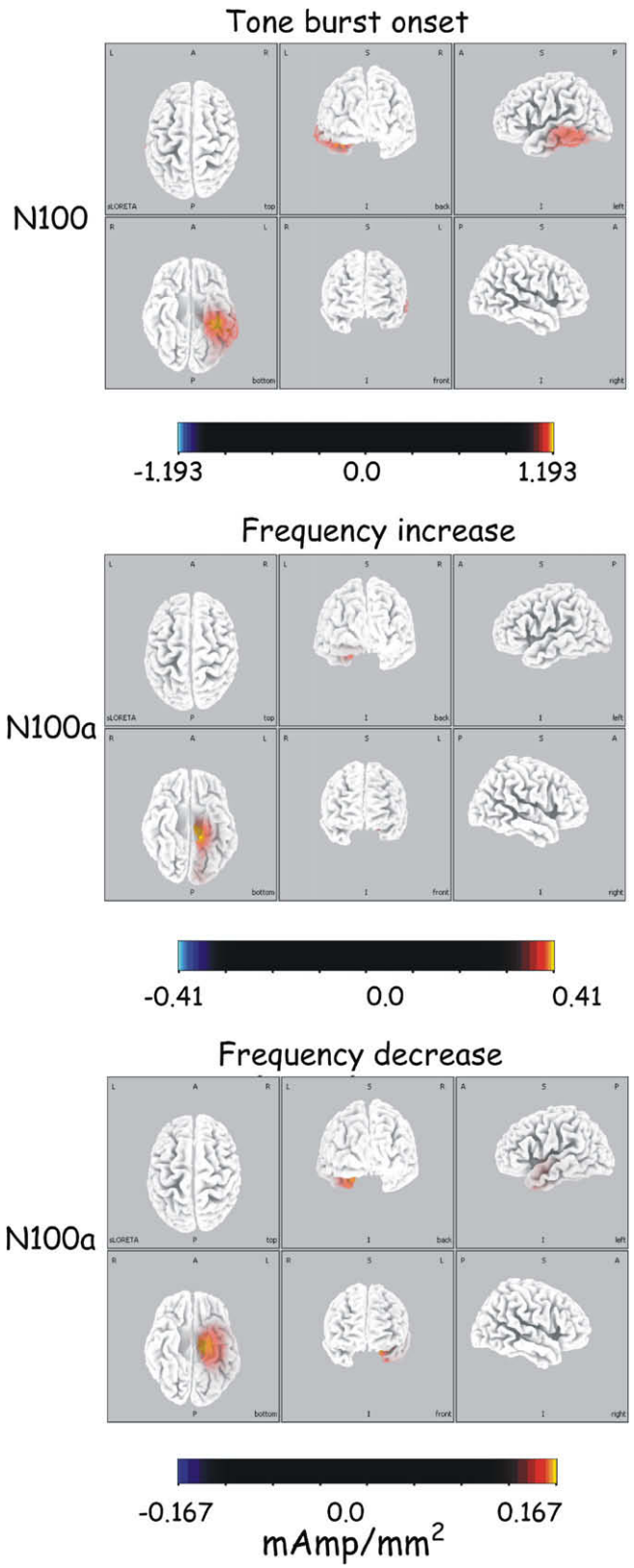

Fig. 8. Average source current density estimates associated with N_{100} to burst onset (top) and with N_{100a} to frequency increase from 250 to 375 Hz (middle) and decrease from 375 to 250 Hz (bottom). Images are based on grand-averaged waveforms from 15 subjects. Six views of the brain are presented for each component, as indicated on each view. Whereas N_{100} activity to burst onset was in the vicinity of secondary auditory areas in the Temporal lobe, N_{100a} activity to frequency changes were more midline, inferior and somewhat more anterior.

and should not be taken as an absolute and accurate determination of the location of activity.

Furthermore, in our previous study on potentials to frequency change (Dimitrijevic et al., 2008) we used dipole source estimation procedures. These procedures use a different set of assumptions, such as the number of dipoles, their symmetry and distance from a seed location, to converge on a solution. The comparison of source estimation results in the two studies is therefore instructive and revealing, particularly noting that both converged on the same general area of the temporal lobe.

The onset response sources in Fig. 8 are somewhat below the usual location of primary auditory cortex in the superior temporal plane. This slight discrepancy in location of the onset response may be due to the low spatial resolution of the method. However, in earlier studies using noise bursts and speech sounds, N_{100} was located to primary auditory cortex (e.g., Laufer and Pratt, 2003b; Sinai and Pratt, 2003). This indicates that the source estimation method and the number of electrodes used provide valid results, and the discrepancy between onset response and change response source locations reflects a real difference. Moreover, regardless of the precise location of the sources, the differences among onset and change responses hold because the same source estimation transformations were used on the waveforms. The differences in distribution of brain activity to sound onset and to frequency change found here are compatible with earlier findings. Using different source estimation techniques and avoiding the spectral confound of sound onset, the N_{100} to frequency change had a dipole source anterior and inferior to that of the N_{100} to stimulus onset (Krumbholz et al., 2003). Animal data also suggest that complex stimuli activate regions outside the auditory cortex core (Tian et al., 2001). Coupled with the opposite dipole orientations in our previous study compared to an earlier study on onset responses (Verkindt et al., 1995) all these results suggest that the N_{100a} to frequency change is different than N_{100} to tone burst onset.

4.1. Comparisons with our previous frequency change study

In our previous study (Dimitrijevic et al., 2008) each frequency change was a brief frequency increase which was promptly (after 100 ms) followed by return to the base frequency of a continuous tone. The present study used much longer (1 s) delays between frequency increase and decrease and base frequency was presented as tone bursts that lasted a few seconds each, rather than a continuous tone. These differences in stimuli enabled separation of the responses to frequency increase and decrease in this study (see Section 4.3). In addition the base frequency (high or low) from which the change took place could be randomly presented.

In this study, N_{100} to frequency change was double-peaked in the lateral electrodes, whereas in the previous study N_{100} was single-peaked in the midline electrodes, while no lateral electrodes were studied. This difference between studies in N_{100} morphology may therefore be attributed to the different electrodes analyzed. We have previously shown that stimulus offset evoked a double-peaked N-Complex with an N_{100b} that is unique to sound offset (Michalewski et al., 2005; Pratt et al., 2005, 2007). One might suggest that in the present study, with sound offsets at the end of each tone burst, the generators of the offset N_{100b} were excited, resulting in an N_{100b} to frequency change. In contrast, in the previous study a continuous tone was used and no offsets occurred. However, the sources of N_{100b} and N_{100a} of this study, although somewhat differently lateralized, were not significantly different, contrasting with N_{100a} and N_{100b} to sound offset which are distinct in laterality (Pratt et al., 2005; Pratt et al., 2007). It is therefore highly unlikely that N_{100b} to frequency change is homologous to its counterpart to sound offset. The single-peaked N_{100} of our previous frequency change study may have resulted from destructive

summation of responses to frequency increase and decrease, which may also explain the diminished P_{200} observed in the previous study.

The diminished P_{200} in the previous study was suggested to result from temporal overlap with the negative SN. In this study, a double-peaked N_{100} was noted, as compared to a single-peaked N_{100} in the previous study. These differences may suggest that in the previous study N_{100a} to frequency decrease and P_{200a} to increase coincided resulting in a smaller amplitude P_{200} and a single-peaked N_{100}, corresponding to this study's N_{100b}-to-frequency decrease. In the previous study, we also noted that the diminished P_{200} had a single peak with the 250-Hz base frequency but it was double-peaked with 4000 Hz. We then suggested that the double-peaked P_{200} may represent a composite of the response to the frequency increase and the promptly following frequency decrease and that the second P_{200} peak may therefore represent the P_{200} of the decrease response. In this study, with frequency increase and decrease temporally removed by an entire second, we found a larger and split P_{200} to both frequency increase and frequency decrease, with both base frequencies. Moreover, the source current density distributions of P_{200a} and P_{200b} were often significantly different. This does not support the suggestion that P_{200} double peaking was a composite of homologous components to frequency increase and the following decrease. Noting that in the present study P_{200a} was appreciably more robust with 250 Hz, suggests that in the previous study the larger P_{200a} with 250 Hz may have overwhelmed the following smaller P_{200b}, obscuring its peak. All these findings indicate that the double-peaked P_{200} to both frequency increase and to frequency decrease is a composite of two distinct components, the first of which may overwhelm the second, resulting in a single-peaked P_{200} under some conditions.

The results of this study showed significant effects of base frequency on the amplitude of SN, which was larger to changes from the high-base frequency. These effects were not evident in our previous study. In addition to the differences in the acoustic stimuli of the two studies, this difference may be attributed to the method of measuring SN amplitude. In the previous study, SN amplitude was measured after filtering with a band pass of 0.05–5 Hz and averaging the amplitude between 300 and 600 ms. In this study, we did not filter out above 5 Hz and measured SN peak amplitude as well as the average amplitude from the peak to 900 ms, emphasizing peak amplitude and its contribution to average amplitude measures.

In our previous study, the dipole sources of N_{100} were larger in auditory cortex of the right hemisphere. In this study, source current densities were predominantly in right temporo-parietal areas for N_{100b} to frequency decrease and were bilateral or even on the left for N_{100a}. It therefore would appear that N_{100} of the previous study was homologous to N_{100b} to frequency decrease of this study. However, in this study N_{100a}amplitude to frequency increase was significantly affected by the magnitude of increase only with the low-base frequency, similar to the findings of the previous study. All this suggests that the N_{100} of the previous study was a composite of the N_{100a} and N_{100b} to frequency increase and decrease of this study.

4.2. Comparison of potentials to high- and low-base frequencies

The differences between brain responses to low- and high-base frequency confirm our findings in the previous study (Dimitrijevic et al., 2008) and are in line with the different modes of encoding high and low frequencies ('place principle' vs 'volley principle', respectively). In the previous study, these differences were demonstrated by slope analysis, across a larger number of change magnitudes, while in this study only two levels of change magnitude were available so analysis of variance was used and indicated similar effects. Similar to our previous study (Dimitrijevic et al., 2008), components were often larger in amplitude and earlier with the large (50%) than with the small (10%) frequency change, with the effect more evident when change was from the low-(250 Hz) base frequency. In our previous study we attributed the longer latencies in response to the low-frequency changes to a temporal window of a necessary number of cycles to detect frequency change. Such a window of a set number of cycles is inherently longer for low frequencies because of the longer duration of each cycle.

Furthermore, in this study, components were sometimes larger in amplitude but later in response to the large (50%) than to the small (10%) frequency increase with the high-(4000 Hz) base frequency. In contrast, frequency decrease evoked components that were also larger but earlier for the 50% change than for the 10% change for both base frequencies. In addition to the difference between frequency increase and decrease, the former findings reflect the difference in central processing of high and low frequencies. Some of the differences between high- and low-base frequency were not observed in our previous study, probably due to the stimuli used: The previous study's short (100 ms) interval between frequency increase and decrease may have resulted in diminished differences between high- and low-base frequency in the composite response to frequency increase and decrease. This is particularly expected with effects that were unique to either frequency increase or decrease, and certainly with effects that were opposite with increase and decrease (e.g., N_{100b} latency to changes from low-base frequency).

In our previous study on frequency change (Dimitrijevic et al., 2008) the dipole sources of N_{100} to frequency change were localized to auditory cortex and differed in location between high- and low-base frequencies. Significant location differences were seen between 250 and 4000 Hz in the medio-lateral direction and in the superior–inferior direction. In contrast to waveform peak amplitudes, dipole magnitudes did not differ between 250 and 4000 Hz. In this study, current densities associated with both constituents of N_{100} were also located to the temporal lobe, particularly in the vicinities of auditory areas, but their distributions were not significantly different between high- and low-base frequency. These results, using no constraints on the number and location of sources, corroborate the previous study's results using a dipole source model, that processing change in high and low frequencies involves the same general brain areas. But differences in source distributions between high- and low-base frequency may be too subtle to detect by smoothed current density distributions (sLORETA) using only 21 channels (this study), compared to dipole estimations with 64 channels (previous study).

The encoding of low and high frequencies in the ascending auditory pathway follows the 'volley principle' and the 'place principle', respectively. The temporal pattern of firing of low-frequency auditory nerve units tends to 'phase lock' to the stimulus waveform. Such phase locking is impaired in conditions such as demyelinating diseases and Auditory Neuropathy (also known as Auditory Dys-synchrony) that affect neural synchrony. Brain potentials to low- and high-frequency changes may therefore be helpful to the differential diagnosis of Auditory Neuropathy from other forms of sensory neural hearing loss, because Auditory Neuropathy patients are impaired in detecting low but not high frequency pitch changes (Zeng et al., 1999).

4.3. Comparison of potentials to frequency increase and decrease

The direction of frequency change (increase or decrease) affected the brain potentials to the change differently, depending on the base frequency and magnitude of frequency change. Moreover, N_{100a} amplitude with the low-base frequency and SN average amplitude for both the high and low-base frequency, were affected

by a significant interaction of direction of change and electrodes, indicating that their scalp distributions varied between frequency increase and decrease. These effects indicate different distributions of brain activity between directions of change, with an early (N_{100}) difference between directions of change that is limited to the low frequencies, and a later (SN) difference between processing of frequency increase and decrease across both high and low frequencies.

Source estimation indicated a significantly larger current density to frequency increase during the time of peak N_{100a} in right frontal areas, but otherwise similar distributions of activity throughout the duration of processing frequency increase and decrease. The different source current density distribution between frequency increase and decrease only during N_{100a} is consistent with the waveform differences observed at that time. The localization of the difference to frontal areas at this latency indicates early associative or cognitive, rather than primarily auditory, differences between processing of frequency increase and decrease.

4.4. Processes associated with potentials to frequency change

The main components in response to both frequency increase and decrease were P_{50}, N_{100}, P_{200}, and SN, with N_{100} and P_{200} often including two peaks each. The double peaking of N_{100} has been previously described in response to short gaps in noise and to sound offset (Michalewski et al., 2005; Pratt et al., 2005, 2007). This may suggest that the bifid N_{100} to frequency change reflects brain processes associated with the termination of one frequency and the onset of another. Cortical activity associated with the N_{100}-to-noise offset was located (Pratt et al., 2005, 2007) bilaterally in temporo-parietal regions, with significant laterality differences between N_{100a} and N_{100b}. In contrast, the sources of N_{100a} and N_{100b} to frequency change in this study were not significantly different and also involved Limbic and Temporal areas. Moreover, whereas P_{50} to sound offset was absent (Pratt et al., 2008), it was present to both frequency increase and decrease, suggesting that frequency change and sound offset evoke different processes in the brain. The bifid N_{100} to frequency change therefore appears to reflect processing of aspects of change that are different from those to sound offset.

The most likely contributors to the N_{100}–P_{200} potentials of this study are the vertex-maximal C-potentials which were found to be associated with both sequential and spectral streaming (e.g., Jones et al., 1998; Jones and Perez, 2001, 2002; Jones, 2003), as well as transition from a periodic to an aperiodic sound (Ostroff et al., 1998; Martin and Boothroyd, 1999). The C-potentials appear to reflect a mismatch of temporal and spectral attributes, or their combination (periodicity) between the incoming acoustic change and the preceding stream.

Detection of a change in the incoming compared to the previous acoustic stream is basic to speech discrimination. Furthermore, direction of change (increase or decrease in frequency) and base frequency (high or low) are important attributes for prosody and consonant and vowel discriminations in speech. The effects of direction of change and base frequency on brain activity may therefore be related to speech perception. The double-peaked N_{100} that has been described in response to speech signals with long Voice Onset Times (VOT) is in line with this suggestion, even though the two peaks have been attributed to the release burst and to the onset of voicing (Sharma et al., 2000). A similar response pattern was obtained in intracranial recordings from the human cortical surface (Liegeois-Chauvel et al., 1999; Steinschneider et al., 1999) and from animals (Steinschneider et al., 1994).

In auditory speech perception, frequency change chirp-like sounds resembling stop consonants are perceived as phonemes when presented in speech context. When presented in noise, phonemic or morphemic contexts, the very same stimuli evoked specific brain responses, with significant left-laterality evident only in the morphemic condition, at similar latencies (136–155 ms) across conditions (Shtyrov et al., 2005). In the present study, the unique association of N_{100a} and SN with auditory frequency change, brings to mind the N_{170} and N_{250} of expert visual processing, in the context of the well-practiced face recognition (Bentin et al., 1996; Tanaka et al., 2006). In visual object processing a cascaded categorization and identification process has been proposed beginning with expert object definition (e.g., face) reflected by N_{170}, leading to the final identification of a particular familiar item in that category manifesting in N_{250} (Scott et al., 2006; Tanaka et al., 2006). In the specific case of face processing, faces evoked an equally prominent N_{170} which was significantly larger than the ERPs to non-face categories, regardless of attention (Carmel and Bentin, 2002). Thus, similar to visual N_{170} and N_{250}, auditory N_{100a} and SN do not require that the subject attend.

Assuming homology of visual expert processing of faces and auditory expert processing of speech elements, N_{100a} may be associated with the well-practiced categorization of the acoustic change as a speech-relevant frequency change (particularly in the low carrier frequencies). The involvement of Frontal cortex at the time of N_{100a} supports its possible additional cognitive role, compared to the purely auditory processing reflected in N_{100b}. SN would be related to the identification of the frequency change as a particular vowel, consonant or prosody. The complex pattern of effects of base frequency, change magnitude and direction of change on N_{100a} and the relative uniformity of SN across these parameters are compatible with this two-tiered model. This suggestion is also in line with earlier suggestions that in both children and adults, the N_1–P_2 peaks are preferentially sensitive to sound salience while the 'N_2–N_4' peaks are sensitive to sound content features (Čeponienė et al., 2005).

5. Summary

The results of this study show that high and low frequencies are processed differently in the human brain. In addition, differences between brain activity evoked by frequency increase and decrease depend on whether the base frequency is high or low. Many of these effects deviate from the usual coupling of shorter latencies with higher amplitudes that is typically seen with effects of stimulus intensity or abruptness of envelope. These differences indicate that the processing of frequency change is more complex than mere levels of activation and may involve networks differentially tuned to processing high and low frequencies, and frequency increase and decrease. This differential activation by high- and low-frequency stimuli may bear on particular types of hearing disorders affecting low – but not high frequencies, such as Auditory Neuropathy. High frequency change processing is important, and may play a role in consonant and vowel perception and the low frequency modulation may be involved in perception of speech prosody.

Acknowledgements

This study was partially supported by the U.S.–Israel Binational Science Foundation, by Grant DC 02618 from the National Institutes of Health, and by the Rappaport Family Institute for Research in the Medical Sciences.

References

Arlinger S, Elberling C, Bak C, Kofoed B, Lebech J, Saermark K. Cortical magnetic fields evoked by frequency glides of a continuous tone. Electroencephalogr Clin Neurophysiol 1982;54:642–53.

Attias J, Urbach D, Gold S, Shemesh Z. Auditory event related potentials in chronic tinnitus patients with noise induced hearing loss. Hear Res 1993;71:106–13.

Bentin S, Allison T, Puce A, Perez E, McCarthy G. Electrophysiological studies of face perception in humans. J Cogn Neurosci 1996;8:551–65.
Brugge JF, Merzenich MM. Responses of neurons in auditory cortex of macaque monkey to monaural and binaural stimulation. J Neurophysiol 1973;36:1138–58.
Carmel D, Bentin S. Domain specificity versus expertise: factors influencing distinct processing of faces. Cognition 2002;83:1–29.
Čeponienė R, Alku P, Westerfield M, Torkki M, Townsend J. Event-related potentials differentiate syllable and non-phonetic correlate processing in children and adults. Psychophysiology 2005;42:391–406.
Dimitrijevic A, Michalewski HJ, Zeng F-G, Pratt H, Starr A. Frequency changes in a continuous tone: auditory cortical potentials. Clin Neurophysiol 2008;119:2111–24.
Friesen LM, Trembley KL. Acoustic change complexes recorded in adult cochlear implant listeners. Ear Hear 2006;27:678–85.
Fuchs M, Kastner J, Wagner M, Hawes S, Ebersole JS. A standardized boundary element method volume conductor model. Clin Neurophysiol 2002;113:702–12.
Godey B, Schwartz D, de Graaf JB, Liegeois-Chauvel C. Neuromagnetic source localization of auditory evoked fields and intracranial evoked potentials: a comparison of data in he same patients. Clin Neurophysiol 2001;112:1850–9.
Goldberg JM, Brownell WE. Response characteristics of neurons in anteroventral and dorsal cochlear nuclei of cat. Brain Res 1973;64:35–54.
Harris KC, Mills JH, Dubno JR. Electrophysiologic correlates of intensity discrimination in cortical evoked potentials of younger and older adults. Hear Res 2007;228:58–68.
Harris KC, Mills JH, He NJ, Dubno JR. Age-related differences in sensitivity to small changes in frequency assessed with cortical evoked potentials. Hear Res 2008;243:47–56.
Javel E, Mott JB. Physiological and psychophysical correlates of temporal processes in hearing. Hear Res 1988;34:275–94.
Jones SJ. Sensitivity of human auditory evoked potentials to the harmonicity of complex tones: evidence for dissociated cortical processes of spectral and periodicity analysis. Exp Brain Res 2003;150:506–14.
Jones SJ, Perez N. The auditory 'C-process': analyzing the spectral envelope of complex sounds. Clin Neurophysiol 2001;112:965–75.
Jones SJ, Perez N. The auditory C-process of spectral profile analysis. Clin Neurophysiol 2002;113:1558–65.
Jones SJ, Longe O, Vaz Pato M. Auditory evoked potentials to abrupt pitch and timbre change of complex tones. Electrophysiological evidence of 'streaming'? Electroencephalogr Clin Neurophysiol 1998;108:131–42.
Kohn M, Lifshitz K, Litchfield D. Averaged evoked potentials and frequency modulation. Electroencephalogr Clin Neurophysiol 1978;45: 236–43.
Krumbholz K, Patterson RD, Seither-Preisler A, Lammertmann C, Lutkenhoner B. Neuromagnetic evidence for a pitch processing center in Heschl's gyrus. Cereb Cortex 2003;13:765–72.
Laufer I, Pratt H. The electrophysiological net response (F-complex) to spatial fusion of speech elements forming an auditory object. Clin Neurophysiol 2003a;114:818–34.
Laufer I, Pratt H. Evoked potentials to auditory movement sensation in duplex perception. Clin Neurophysiol 2003b;114:1316–31.
Liegeois-Chauvel C, deGraaf JB, Laguitton V, Chauvel P. Specialization of left auditory cortex for speech perception in man depends on temporal coding. Cereb Cortex 1999;9:484–96.
Lutkenhoner B. Single-dipole analyses of the N100m are not suitable for characterizing the cortical representation of pitch. Audiol Neurootol 2003;8:222–33.
Lutkenhoner B, Krumbholz K, Seither-Preisler A. Studies of tonotopy based on wave N100 of the auditory evoked field are problematic. Neuroimage 2003;19:935–49.
Martin BA, Boothroyd A. Cortical, auditory, event-related potentials in response to periodic and aperiodic stimuli with the same spectral envelope. Ear Hear 1999;20:33–44.
Martin BA, Boothroyd A. Cortical, auditory, evoked potentials in response to change of spectrum and amplitude. J Acoust Soc Am 2000;107:2155–61.
McCandless GA, Rose DE. Evoked cortical responses to stimulus change. J Speech Hear Res 1970;13:624–34.
Medwetzky L. Central auditory processing [Chapter 25]. In: Katz J, editor. Handbook of clinical audiology. Philadelphia: Lippincott Williams & Wilkins; 2002. p. 495–509.
Michalewski HJ, Starr A, Nguyen TT, Kong Y-Y, Zeng F-G. Auditory temporal processes in normal-hearing individuals and in patients with auditory neuropathy. Clin Neurophysiol 2005;116:669–80.
Moushegian G, Rupert AL, Stillman RD. Scalp-recorded early responses in man to frequencies in the speech range. Electroencephalogr Clin Neurophysiol 1973;35:665–7.
Nichols TE, Holmes AP. Nonparametric permutation tests for functional neuroimaging: a primer with examples. Hum Brain Mapp 2002;15:1–25.
Ostroff MJ, Martin BA, Boothroyd A. Cortical evoked responses to acoustic change within a syllable. Ear Hear 1998;19:290–7.
Palmer AR. Neural signal processing. In: Moore CJ, editor. Hearing. San Diego: Academic Press; 1995.
Palmer AR, Russel IJ. Phase-locking in the cochlear nerve of the guinea pig and its relation to the receptor potential of inner hair cells. Hear Res 1986;24:1–15.
Pantev C, Hoke M, Lehnertz K, Lutkenhoner B, Anogianakis G, Wittowski W. Tonotopic organization of the human auditory cortex revealed by transient auditory evoked magnetic fields. Electroencephalogr Clin Neurophysiol 1988;69:160–70.
Pantev C, Bertrand O, Eulitz C, Verkindt C, Hampton S, Schuierer G, et al. Specific tonotopic organizations of different areas of the human auditory cortex revealed by simultaneous magnetic and electric recordings. Electroencephalogr clin Neurophysiol 1995;94:26–40.
Pascual-Marqui RD. Standardized low resolution brain electromagnetic tomography (sLORETA): technical details. Methods Find Exp Clin Pharmacol 2002;24D:5–12.
Pascual-Marqui RD, Michel CM, Lehmann D. Low resolution electromagnetic tomography: a new method for localizing electrical activity in the brain. Int J Psychophysiol 1994;18:49–65.
Pratt H, Bleich N, Mittelman N. The composite N_1 component to gaps in noise. Clin Neurophysiol 2005;116:2648–63.
Pratt H, Starr A, Michalewski HJ, Bleich N, Mittelman N. The N1 complex to gaps in noise: effects of preceding noise duration and intensity. Clin Neurophysiol 2007;118:1078–87.
Pratt H, Starr A, Michalewski HJ, Bleich N, Mittelman N. The auditory P50 component to onset and offset of sound. Clin Neurophysiol 2008;119:376–87.
Roberts TPL, Poeppel D. Latency of auditory evoked M100 as a function of tone frequency. NeuroReport 1996;7:1138–40.
Rose JE, Brugge JF, Anderson DJ, Hind JE. Patterns of activity of single auditory nerve fibers of the squirrel monkey. In: De Reuck AVS, Knight J, editors. Hearing mechanisms in vertebrates. London: Churchill; 1968.
Scott LS, Tanaka JW, Sheinberg DL, Curran T. A reevaluation of the electrophysiological correlates of expert object processing. J Cogn Neurosci 2006;18:1453–65.
Sharma A, Marsh CM, Dorman MF. Relationship between N1 evoked potential morphology and the perception of voicing. J Acoust Soc Am 2000;108:3030–5.
Shtyrov Y, Pihko E, Pulvermüller F. Determinants of dominance: is language laterality explained by physical or linguistic features of speech? Neuroimage 2005;27:37–47.
Sinai A, Pratt H. High-resolution time course of hemispheric dominance revealed by low-resolution electromagnetic tomography. Clin Neurophysiol 2003;114:1181–8.
Steinschneider M, Schroeder CE, Arezzo JC, Vaughan HG. Speech-evoked activity in primary auditory cortex: effects of voice onset time. Electroencephalogr Clin Neurophysiol 1994;92:30–43.
Steinschneider M, Volkoc I, Noh M, Garell P, Howard MT. Temporal encoding of the voice onset time phonetic parameter by field potentials recorded directly from human auditory cortex. J Neurophysiol 1999;82:2346–57.
Stufflebeam SM, Poeppel D, Rowley HA, Roberts TPL. Peri-threshold encoding of stimulus frequency and intensity in the M100 latency. NeuroReport 1998;9:91–4.
Talairach J, Tournoux P. Coplanar stereotaxic atlas of the human brain. Stuttgart: Thieme; 1988.
Tanaka JW, Curran T, Porterfield AL, Collins D. Activation of preexisting and acquired face representations: the N250 event-related potential as an index of face familiarity. J Cogn Neurosci 2006;18:1488–97.
Tervaniemi M, Just V, Koelsch S, Widmann A, Schroger E. Pitch discrimination accuracy in musicians vs nonmusicians: an event-related potential and behavioral study. Exp Brain Res 2005;161:1–10.
Tian B, Reser D, Durham A, Kustov A, Rauschecker JP. Functional specialization in rhesus monkey auditory cortex. Science 2001;292:290–3.
Verkindt C, Bertrand O, Perrin F, Echallier J-F, Pernier J. Tonotopic organization of the human auditory cortex: N100 topography and multiple dipole model analysis. Electroencephalogr Clin Neurophysiol 1995;96:143–56.
Whitfield IC, Evans EF. Responses of auditory cortical neurons to stimuli of changing frequency. J Neurophysiol 1965;28:655–72.
Yingling CD, Nethercut GE. Evoked responses to frequency shifted tones: tonotopic and contextual determinants. Int J Neurosci 1983;22:107–18.
Zeng F-G, Oba S, Garde S, Sininger Y, Starr A. Temporal and speech processing deficits in auditory neuropathy. NeuroReport 1999;10:3429–35.